2025 IEEE Conference on Control Technology and Applications (CCTA)
August 25 - 27, 2025. San Diego, CA, USA

GNN-Based Surrogate Model for Reconfigurable Battery Packs

Ali Irshayyid, *Graduate Student Member, IEEE* and Jun Chen, *Senior Member, IEEE*

***Abstract*— This paper presents a novel Graph Neural Network (GNN)-based surrogate model for predicting state evolution in reconfigurable battery packs. By leveraging graph-based representations of battery cell interconnections, the proposed approach addresses the unique challenge of estimating the imbalance in state-of-charge (SOC) and temperature of cells of a battery pack in dynamic battery configurations. Unlike conventional methods that focus on instantaneous state estimation, our GNN model predicts future SOC and temperature distributions by considering both current system state and switch configuration. The model architecture combines Graph Attention Networks with pooling operations to effectively capture cell-to-cell interactions and battery pack-level dynamics. Numerical results demonstrate that our GNN-based approach significantly outperforms baseline Feedforward Neural Network (FNN) and FNN-attention models, showing substantial improvements in prediction accuracy for both temperature and SOC while maintaining robust performance even with limited training data.**

I. Introduction

The increasing adoption of electric vehicles (EVs) [1], [2], the integration of renewable energy sources into smart grids [3]–[5], and the growing demand for reliable backup power systems in various applications from mobile devices to electric planes all point to the critical role of battery packs in modern technologies [6]. Lithium-ion battery packs in EVs consist of hundreds of cells arranged in series and/or parallel configurations to meet the high voltage and energy requirements [7]. However, these complex battery systems face challenges in their design and management. A key challenge is cell imbalance, which arises from variations in battery cell characteristics due to manufacturing inconsistencies, uneven aging, and difference in operation conditions [8]–[10]. This can lead to state-of-charge (SOC) and temperature imbalance, which can result in reduced battery pack lifespan, safety issues such as overheating and thermal runaway, and diminished energy efficiency [11]–[15].

While conventional battery management systems employ techniques like cell balancing to mitigate these issues, their effectiveness is often limited by the static nature of cell interconnections. To address these inherent limitations of fixed cell topologies, reconfigurable battery packs, enabled by networks of controllable switches, offer a promising solution [16]–[18]. Consisting of battery cells equipped with switching circuits, reconfigurable battery packs allow dynamic reconfiguration of cell connections in series, parallel, or bypass configurations. Such a reconfigurable architecture enables flexible control over cell interconnections, allowing battery packs to be dynamically configured in different modes such as all-serial, all-parallel, or hybrid (serial-parallel-bypass) arrangements [19]. By dynamically altering the connections between battery cells, reconfigurable battery systems can improve cell balancing, enhance lifespan and safety, and optimize energy efficiency [20], [21].

However, the adoption of reconfigurable battery packs poses significant challenge in their modeling. Existing work on battery modeling has focused on fixed topologies, where the interconnections between cells remain static [22]. These models typically capture electrical and thermal characteristics through equivalent circuits or electrochemical principles. However, reconfigurable battery systems require models that can account for the dynamic nature of cell connections to predict the impacts of different switching configurations on future system states, such as cell-to-cell variations in SOC and temperature distributions.

Attempts have been made in literature to address this issue. For example, in [16], [23], several supervised learning approaches have been investigated to predict optimal topology switches in a reconfigurable battery pack. To generate training data, a multi-objective optimization problem is formulated for the topology selection, with objectives to maximize the sum of all cell SOC values and to minimize the range of SOC values across cells. By solving the multi-objective optimization problem through simulations, the training data is obtained for training various machine learning models to predict the best topology for the next control period. The FNN model achieved the best performance with 72% testing accuracy. While the work of [16], [23] demonstrate the potential for modeling battery pack reconfiguration, it has significant scalability limitations. Exhaustive simulations are required for training data generation, which enumerates all possible transitions between topology pairs. Furthermore, each configuration needs multiple simulations under different conditions to capture the patterns of SOC changes. This approach becomes computationally intractable when the number of cells increases, since the number of possible topologies grows exponentially with pack size.

To scale up for the large number of cells that commonly exist in EVs, we develop a Graph Neural Network (GNN)-based surrogate model for reconfigurable battery packs to predict future variations of SOC and cell temperatures. GNNs are powerful deep learning models designed for processing data represented as graphs, making them particularly suitable for reconfigurable battery packs where cell interconnections can be represented as a graph structure. Our GNN ar-

This work is supported in part by National Science Foundation through Award #2237317.

Ali Irshayyid and Jun Chen are with the Department of Electrical and Computer Engineering, Oakland University, Rochester, MI 48309 USA (e-mail: {aliirshayyid,junchen}@oakland.edu).

2025 IEEE Conference on Control Technology and Applications (CCTA) | 979-8-3315-3908-5/25/$31.00 ©2025 IEEE | DOI: 10.1109/CCTA53793.2025.11151387

chitecture naturally captures the physical connections and operational dynamics of reconfigurable battery packs by representing both battery cells and switches as nodes in a graph, with edges representing their physical connections. The battery cell nodes contain state information such as SOC and temperature, while switch nodes encode the mode of connections between two adjacent cells. By processing this graph-structured data through multiple GNN layers, our model learns to aggregate information from neighboring nodes and predict how different switch configurations affect the evolution of cell states.

The GNN-based surrogate model is trained using simulation data generated from a detailed experimentally-validated electro-thermal battery model that incorporates both electrical equivalent circuits and thermal dynamics [24], capturing the complex interactions between battery cells in various reconfigurable topologies. Numerical results demonstrate that, in all test conditions, the proposed GNN-based surrogate model significantly outperforms traditional FNNs and FNN-attention models in terms of estimation accuracy.

The reminder of the paper is organized as follows. Section II presents the battery pack modeling approach using integrated electro-thermal modeling, while Section III describes the graph representation of the reconfigurable battery pack system. Section IV details the proposed GNN-based surrogate model architecture and Section V outlines the experimental setup and discusses the experimental results. Finally, Section VI concludes the paper and presents future research directions.

II. Dynamics of Battery Packs

A. Cell Dynamics

The cell model adopted in this work is based on the equivalent circuit model (ECM) [24]–[26], which combines an electrical circuit with a two-state thermal model to capture both the electrical and thermal dynamics of lithium-ion batteries. The electrical behavior is characterized by two RC pairs and a series resistance, with dynamics governed by:

$$\dot{V}_1 = -\frac{V_1}{R_1 C_1} + \frac{I}{C_1} \tag{1a}$$

$$\dot{V}_2 = -\frac{V_2}{R_2 C_2} + \frac{I}{C_2} \tag{1b}$$

$$v = V_{OC} - V_1 - V_2 - I R_o, \tag{1c}$$

where v is the terminal voltage, V_{OC} is the open-circuit voltage, and I is the current (positive for discharge, negative for charge). The RC pairs are characterized by voltages V_1, V_2, resistance R_1, R_2, and capacitance C_1, C_2, with R_o representing the series resistance. The cell's SOC is govern by:

$$\dot{s} = -\frac{\eta}{3600 C_n} I, \tag{2}$$

where s is the state-of-charge, η is the coulombic efficiency and C_n is the nominal capacity of the cell in Amp-Hour.

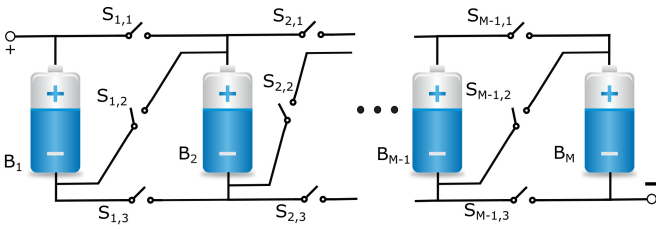

Fig. 1. Reconfigurable battery packs consisting of M cells.

The thermal behavior is modeled using core and surface temperatures:

$$C_c \dot{T}_c = Q + \frac{T_s - T_c}{R_c} \tag{3a}$$

$$C_s \dot{T}_s = \frac{T_c - T_s}{R_c} + \frac{T_f - T_s}{R_u}, \tag{3b}$$

where T_c is the core temperature, T_s is the surface temperature, T_f is the ambient temperature, C_c and C_s are the heat capacities of the core and surface respectively, R_c is the conduction resistance between T_c and T_s, while R_u is the convection resistance between T_f and T_s. The heat generation Q is given by:

$$Q = I(V_{oc} - v) - I\frac{T_s + T_c}{2}\frac{dV_{oc}}{dT}. \tag{4}$$

All model parameters (V_{oc}, R_o, R_1, R_2, C_1, C_2) are functions of SOC s and temperatures T_c and T_s, and can be expressed as:

$$\sigma = f_\sigma(s, T_c, T_s), \tag{5}$$

where $\sigma = \{V_{oc}, R_o, R_1, R_2, C_1, C_2\}$. In this paper, parameters in [24], which have been experimentally validated, are adopted for a nominal battery cell.

B. Battery Reconfiguration

These individual cell models are integrated into a reconfigurable battery pack consisting of M cells interconnected through a network of switches. As shown in Fig. 1, a three-switch-per-connection architecture is adopted in this paper, where switches can be either open or closed, enabling dynamic formation of series and parallel connections between adjacent cells. This architecture provides sufficient degrees of freedom for topology reconfiguration while avoiding the limited flexibility of two-switch designs or the excessive complexity of four-switch arrangements.

Formally, let $\mathcal{B}$ be a battery pack with M cells $(B_1, B_2, ..., B_M \in \mathcal{M})$ connected through a network of switches as shown in Fig. 1, where each cell B_i has three switches $(S_{i,1}, S_{i,2}, S_{i,3})$ controlling its configuration. In other words, the switch configuration for cells B_i, $i = 1, \ldots, M-1$ determines its connection state sw_i with its adjacent cell B_{i+1}, with the following notation:

$$sw_i = \begin{cases} 1 & \text{for series connection between } B_i \text{ and } B_{i+1} \\ 0 & \text{for parallel connection between } B_i \text{ and } B_{i+1}. \end{cases}$$

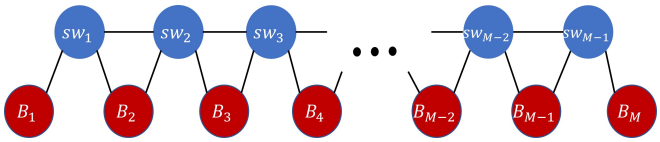

Fig. 2. Graph representation of a reconfigurable battery pack with M cells.

Finally, the dynamics of each cell B_i is given by (1)-(5). Given a prediction horizon τ, we define the SOC and temperature imbalance across cells as:

$$\Delta s = \max_{1\le i\le M} s_i(\tau) - \min_{1\le i\le M} s_i(\tau) \tag{6a}$$

$$\Delta T_c = \max_{1\le i\le M} T_{c,i}(\tau) - \min_{1\le i\le M} T_{c,i}(\tau). \tag{6b}$$

Note that here the temperature imbalance is defined over the core temperature T_c only. However, the work presented in this paper can be straightforwardly extended to the case of T_s.

III. Graph Representation of Cell Topologies

Reconfigurable battery packs can be naturally represented as a graph structure that captures both the physical connectivity and the operational states of the system. As illustrated in Fig. 2, we model switches and battery cells as different types of nodes, where their interactions and physical connections are represented by edges. The switches, which control the series-parallel configurations, are represented as one type of node carrying binary state information. The battery cells form another type of nodes, containing their respective state variables such as s and T_c. The physical layout of battery packs determines the edge connections. For the reconfigurable battery pack shown in Fig. 1, edges exist between adjacent switches and between switches and their connected battery cells. Such a graph-based approach effectively captures the dynamic reconfigurability of the battery pack and allows us to model how the switch states influence the electrical configuration of the battery pack.

Formally, we define our graph structure as follows. Let $G = (V, E)$ be an undirected graph representing the battery pack structure, where V is the set of nodes and E is the set of edges. The node set V consists of two disjoint subsets: $V = V_s \cup V_b$, where $V_s = \{v_1, v_2, ..., v_{M-1}\}$ represents the set of switch nodes and $V_b = \{v_1, v_2, ..., v_M\}$ represents the set of battery cell nodes. Each node $v_i \in V$ carries features such as switch status for $v_i \in V_s$ and SOC for $v_i \in V_b$. We denote the feature for node v_i as x_{v_i}. More details of the features will be given in Section V-A. The edge set E represents physical connections, i.e., $E = \{(i,j)|$ node i is physically connected to node $j\}$. The adjacency matrix $A = [A_{ij}] \in \mathbb{R}^{|V|\times|V|}$ is defined as:

$$A_{ij} = \begin{cases} 1 & \text{if } (i,j) \in E \\ 0 & \text{otherwise.} \end{cases} \tag{7}$$

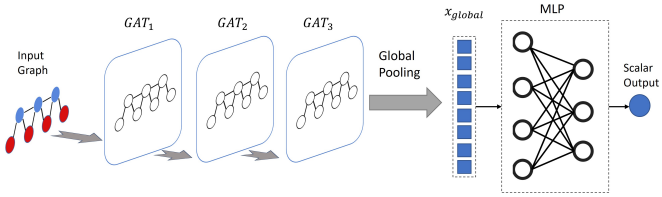

Fig. 3. GNN model architecture used in this paper.

IV. GNN-based Surrogate Model

GNNs have emerged as powerful architectures for modeling complex systems with dynamic relationships. For reconfigurable battery pack modeling, several GNN variants such as Graph Convolutional Networks (GCNs) [27] and Graph Attention Networks (GATs) [28] can be considered. While GCNs offer a straightforward approach to aggregate neighbor information using fixed weights based on graph structure, GATs dynamically assign different levels of importance to neighboring nodes using an attention mechanism. This property is particularly crucial for reconfigurable battery packs, where the influence of one cell on another can vary significantly based on their electrical connection state. Therefore, GATs are used in this paper. In the remaining of this paper, we use "GNNs" and "GATs" interchangeably for our modeling approach.

Given SOC variation Δs and temperature variation ΔT_c as defined in (6), the goal of the GNN-based surrogate modeling is to learn and predict Δs and ΔT of battery cells while accounting for the dynamic reconfigurable topology. The proposed GAT architecture is shown in Fig. 3, which consists of three GAT layers that process both the battery cell and switch node features while leveraging the graph structure defined in Section III. The input of the first GAT layer is the original nodes features, $\mathbf{x} = \{\vec{x}_1, \vec{x}_2, ..., \vec{x}_{|V|}\}, \vec{x}_i \in \mathbb{R}^F$, where F is the number of features in each node. After the message passing process, new node features are produced as the output of this layer, denoted as $\mathbf{x}' = \{\vec{x}'_1, \vec{x}'_2, ..., \vec{x}'_{|V|}\}, \vec{x}'_i \in \mathbb{R}^{F'}$, where F' represents the embedding size.

In each GAT layer, the first step is to transform the features of each node into a high-level representation parametrized by $\mathbf{W} \in \mathbb{R}^{F'\times F}$. After that, a self-attention operation is applied at every node as follows:

$$\alpha_{ij} = \frac{\exp\left(\text{LeakyReLU}\left(\vec{a}_1^T \mathbf{W}\vec{x}_i + \vec{a}_2^T \mathbf{W}\vec{x}_j\right)\right)}{\sum_{k\in\mathcal{N}_i\cup i}\exp\left(\text{LeakyReLU}\left(\vec{a}_1^T \mathbf{W}\vec{x}_i + \vec{a}_2^T \mathbf{W}\vec{x}_k\right)\right)},$$

where α_{ij} is the normalized attention coefficients representing the importance of node j's features to node i, $\mathcal{N}_i$ is a set of i's node neighbors, and $\vec{a} \in \mathbb{R}^{2F'}$ is the attention learnable weight vector. The final output features for each node are determined by computing a linear combination of the features using the normalized attention coefficients. After the GAT layers transform the node features, global pooling is employed to form a fixed-sized representation. The fixed-representation is then processed through FNN layer to produce a scalar output.

V. Numerical Results

A. Experimental Setup and Data Generation

We simulated a ten-cell reconfigurable pack with heterogeneous capacities. The 2^9 series/parallel combinations yield 512 unique topologies. For each topology, we executed 10 trials (5120 runs total) with random initial conditions: $T_c \in [17.5, , 27.5]^{\circ}\mathrm{C}$ and $\mathrm{SOC} \in [0.8, , 1.0]$. Each 500 s discharge at 1.5 A produced final Δs and ΔT_c (see (6)).

Two GNN-based surrogate models are investigated, each with different features for the battery cell nodes. In the first scenario, only the battery states such as s_i and $T_{c,i}$ are used as input features in the battery cell node, with s_i being used when the goal is to predict Δs and $T_{c,i}$ being used when the goal is to predict ΔT_c. In the second scenario, the discharge current of individual battery cell is added as an additional input feature. In both scenarios, the switch status sw_i is used as an input feature for the switch node, as discussed in Section III. The final Δs and ΔT_c measurements serve as the target variables for both models.

For benchmarking, two approaches are considered: (1) a four-layer FNN with ReLU activation that processes flattened battery cell states and switch configurations [16], and (2) our previously developed FNN-attention model with four attention heads for capturing cell-to-cell interactions [29]. The FNN-attention model first extracts features through a linear layer with normalization, then applies multi-head self-attention to dynamically weigh the importance of different battery cells and their interconnections. A residual connection preserves individual cell information alongside relational data before a final linear layer generates predictions.

B. Results and Discussions

Our evaluation metrics include Root Mean Squared Error (RMSE), which quantifies prediction accuracy with lower values indicating better performance, and Mean Absolute Percentage Error (%), which provides a relative measure of prediction error as a percentage of the true value. The percentage error metric is particularly valuable for comparing prediction accuracy across different scales of measurements, such as between ΔT_c and Δs predictions. The evaluation is conducted using different percentages of training data (50%, 30%, and 10%) to assess model robustness under limited data availability. Results are presented under two scenarios: (Case I) without individual cell currents as an input feature (Table I) and (Case II) with individual cell currents as input feature (Table II).

For temperature prediction, the proposed GNN-based model demonstrates superior performance across all training data configurations. As shown in Table I, GNN achieved RMSE values of 0.094, 0.109, and 0.223 for 50%, 30%, and 10% training data respectively, significantly outperforming both FNN and FNN-attention models. In the second experiment, the individual cell current is included as an additional input feature, the GNN's performance improved further, achieving RMSE values of 0.074, 0.1, and 0.173 across the three training data configurations. This improvement suggests that the GNN effectively leverages the additional current information to enhance prediction accuracy.

For SOC prediction, the results followed a similar pattern, with the proposed GNN-based model demonstrating consistently superior performance. In Case I, the GNN achieved RMSE values of 0.02, 0.02, and 0.023 for 50%, 30%, and 10% training data respectively. These results represent a substantial improvement over both the FNN and FNN-attention models. Similarly, in the second experiment where the individual cell current is included as an input, the GNN model performance improved further, with RMSE values reducing to 0.015, 0.015, and 0.019 across the three training configurations. Notably, the GNN architecture maintained robust performance even with limited training data (10%), demonstrating its effectiveness in scenarios where extensive training data may not be available.

Fig. 4 provides a visual comparison of the proposed GNN-based model's percentage errors for both ΔT_c and Δs predictions across different training data percentages. In Fig. 4 (Case I), we observe that Δs prediction errors show a gradual increase as training data decreases, ranging from 10.46% with 50% training data to 12% with 10% training data. The ΔT_c prediction errors follow a similar trend but with notably lower error rates, increasing from 1.9% to 4.4% as training data is reduced. With individual cell currents as input feature, Fig. 4 (Case II) demonstrates improved performance, particularly for Δs predictions, with errors decreasing to 7.7% with 50% training data. This improvement can be attributed to the addition of discharge current as an input feature, which either needs to be measured for each cell or needs to be calculated using the network topology [30] (hence requiring additional complexity for real-time implementation).

The performance advantage of the GNN over baseline models was most evident in temperature prediction, where the GNN achieved significantly lower errors across both metrics - with RMSE values ranging from 0.094 to 0.223 and percentage errors between 1.9% and 4.4%, compared to both FNN (RMSE: 0.357-0.44, percentage errors: 7.14-8.75%) and FNN-attention models (RMSE: 0.393-0.453, percentage errors: 8.19-9.20%) across all training conditions. The superior performance of the GNN can be attributed to its ability to effectively capture the complex relationships between battery cells in the reconfigurable battery pack structure. Furthermore, the addition of individual cell current as an input feature provides valuable information about the battery topology, enabling the model to better capture the behavior of the battery pack. However, as discussed earlier, it requires extra computation or sensors to obtain individual cell currents for real-time implementation.

C. Generalization to Unseen Configurations

While the previous results demonstrate strong performance across different training data percentages, the generalization to unseen configurations is not tested. In other words, in the previous evaluations, both training data and test data are randomly sampled from the entire dataset, giving the surrogate

TABLE I

MODEL PERFORMANCE COMPARISON (CASE I)

Model	50% Training		30% Training		10% Training	
	RMSE	%	RMSE	%	RMSE	%
ΔT_c						
FNN	0.357	7.14	0.378	7.61	0.440	8.75
FNN-attention	0.393	8.19	0.459	9.30	0.453	9.20
GNN (Proposed)	**0.094**	**1.90**	**0.109**	**2.20**	**0.223**	**4.40**
Δs						
FNN	0.026	13.37	0.028	14.00	0.033	16.56
FNN-attention	0.026	13.42	0.028	14.48	0.034	17.77
GNN (Proposed)	**0.020**	**10.46**	**0.020**	**10.80**	**0.023**	**12.00**

TABLE II

MODEL PERFORMANCE COMPARISON (CASE II)

Model	50% Training		30% Training		10% Training	
	RMSE	%	RMSE	%	RMSE	%
ΔT_c						
FNN	0.361	7.21	0.378	7.62	0.471	9.42
FNN-attention	0.414	8.30	0.434	8.90	0.567	11.93
GNN (Proposed)	**0.074**	**1.49**	**0.10**	**2.20**	**0.173**	**3.70**
Δs						
FNN	0.028	14.08	0.03	15.54	0.033	17.00
FNN-attention	0.03	16.14	0.0316	17.25	0.034	18.17
GNN (Proposed)	**0.015**	**7.7**	**0.015**	**8.07**	**0.019**	**10.10**

TABLE III

PREDICTIONS FOR UNSEEN CONFIGURATIONS (CASE I)

Model	50% Training		30% Training		10% Training	
	RMSE	%	RMSE	%	RMSE	%
ΔT_c						
FNN	0.316	6.47	0.346	7	0.458	9.4
FNN-attention	0.397	8.31	0.440	8.9	0.563	11.68
GNN (Proposed)	**0.122**	**2.21**	**0.109**	**2.24**	**0.212**	**4.3**
Δs						
FNN	0.026	14.28	0.028	14.43	0.034	17.83
FNN-attention	0.026	12.98	0.026	14.16	0.037	18.92
GNN (Proposed)	**0.02**	**11.25**	**0.022**	**12.42**	**0.022**	**11.20**

TABLE IV

GENERALIZATION FOR UNSEEN CONFIGURATIONS (CASE II)

Model	50% Training		30% Training		10% Training	
	RMSE	%	RMSE	%	RMSE	%
ΔT_c						
FNN	0.311	6.18	0.368	7.29	0.489	9.81
FNN-attention	0.374	7.49	0.447	8.67	0.565	11.18
GNN (Proposed)	**0.1**	**2.02**	**0.109**	**2.24**	**0.151**	**3**
Δs						
FNN	0.028	14.44	0.031	16.63	0.034	18.40
FNN-attention	0.028	14.37	0.033	17.05	0.037	16.60
GNN (Proposed)	**0.014**	**7.59**	**0.017**	**9.8**	**0.02**	**10.18**

models opportunity to train over all possible configurations. Though this is not an issue for a small battery pack, it may not be feasible to collect data for all configurations when the number M of cells increases.

In this section, we randomly select 51 configurations (10% of the total 512 possible configurations) and reserved them exclusively for testing, ensuring these configurations were never seen during training. From the remaining 4610 samples, we created three training scenarios using 50% (2305 data samples), 30% (1536 data samples), and 10% (461 data samples) of the data. It's important to note that when creating training dataset (for 50%, 30%, and 10%), data are sampled randomly (from the remaining 4610 samples) regardless of its configuration features. Tables III and IV present the models' performance on unseen configurations with and without the individual cell current as an input, respectively. The results demonstrate that while some models show some performance degradation when tested on completely unseen configurations, the GNN model maintains significantly better performance compared to the baseline approaches.

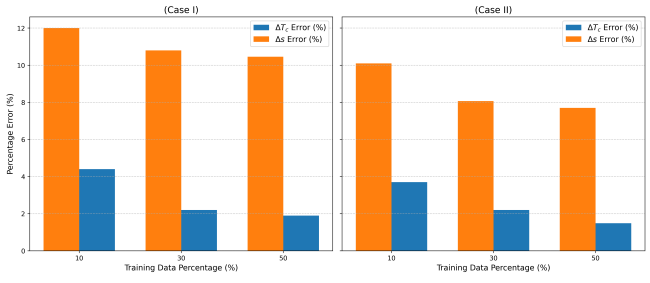

Fig. 4. Comparison of percentage errors for ΔT_c and Δs predictions by the proposed GNN-based surrogate model with respect to training data percentages.

For Case I, without individual cell current as an input feature (Table III), the GNN model achieves remarkable temperature prediction accuracy with RMSE values of 0.122, 0.109, and 0.212 across the three training scenarios, significantly outperforming both FNN and FNN-attention models. The GNN's percentage errors for temperature prediction remain consistently low, ranging from 2.21% to 4.3%, while baseline models show errors up to 11.68%. For Case II with individual cell current (Table IV), the GNN's superior performance becomes even more evident. For temperature prediction, the GNN maintains excellent accuracy with RMSE values of 0.1, 0.109, and 0.151, while baseline models show considerably higher errors. Particularly noteworthy is the GNN's performance in SOC prediction in Case II, where it achieves remarkably low percentage errors (7.59%, 9.8%, 10.18%) compared to the baseline models (14.44%-18.40%).

D. Comparison of Computational Requirements

This section discusses the architectural characteristics and computational requirements of the three models. The GNN model has a moderate number of parameters (24337) compared to the FNN (25185) and FNN-attention (21009) models. While the FNN uses a simple architecture with four layers of decreasing dimensions (256, 64, 16, 1), and the FNN-attention model employs an embedding size of 52 with 4 attention heads, the GNN achieves superior performance using an embedding dimension F' of 24 and 4 attention heads. However, the GNN does require longer training time (87.77 minutes for 50% training data) compared to the FNN (27.45 minutes) and FNN-attention model (31.61 minutes) when trained on an NVIDIA RTX 3070 Ti GPU.

VI. Conclusion

This paper introduces a novel Graph Neural Network (GNN)-based surrogate model for predicting state evolution in reconfigurable battery packs. The proposed model utilizes the graph representation of the reconfigurable battery pack by modeling both cells and switches as different types of nodes connected by edges representing their physical connections. Our approach successfully addresses the challenges of modeling both SOC and temperature imbalance in dynamic battery configurations by leveraging the natural graph structure of the battery pack topology. The proposed GNN architecture demonstrates superior performance compared to traditional Feedforward Neural Networks (FNN) and FNN-attention approaches. The model shows particularly strong performance in temperature prediction, where it achieves significantly lower RMSE values across different training data conditions. Additionally, the incorporation of individual cell current as an input feature further enhances the model's predictive capabilities. The effectiveness of our approach is maintained even with limited training data (10%), demonstrating the model's robustness and potential for practical applications where extensive datasets may not be available. The generalizability is demonstrated by testing the model performance over unseen battery configurations.

References

[1] A. Beaudet, F. Larouche, K. Amouzegar, P. Bouchard, and K. Zaghib, "Key challenges and opportunities for recycling electric vehicle battery materials," *Sustainability*, vol. 12, no. 14, p. 5837, 2020.

[2] J. Chen, A. Behal, and C. Li, "Active cell balancing by model predictive control for real time range extension," in *IEEE Conference on Decision and Control*, Austin, TX, USA, December 13–15, 2021.

[3] M. Ibrahim and R. Elhafiz, "Security analysis of smart grids," *Security and Communication Networks*, vol. 2022, no. 1, p. 7199301, 2022.

[4] M. Ibrahim and A. Alkhraibat, "Resiliency assessment of microgrid systems," *Applied Sciences*, vol. 10, no. 5, p. 1824, 2020.

[5] J. Chen and H. E. Garcia, "Economic optimization of operations for hybrid energy systems under variable markets," *Applied Energy*, vol. 177, pp. 11–24, September 2016.

[6] F. Yang, F. Gao, B. Liu, and S. Ci, "An adaptive control framework for dynamically reconfigurable battery systems based on deep reinforcement learning," *IEEE Transactions on Industrial Electronics*, vol. 69, no. 12, pp. 12 980–12 987, 2022.

[7] "Chevrolet Bolt EV - 2021," accessed on October 8, 2021. [Online]. Available: https://media.chevrolet.com/media/us/en/chevrolet/vehicles/bolt-ev/2021.tab1.html

[8] M. Dubarry, N. Vuillaume, and B. Y. Liaw, "Origins and accommodation of cell variations in li-ion battery pack modeling," *Int. J. of Energy Research*, vol. 34, no. 2, pp. 216–231, 2010.

[9] Q. Zhou, D. Anderson, and J. Sun, "State of health estimation for battery modules with parallel-connected cells under cell-to-cell variations," *eTransportation*, vol. 22, p. 100346, 2024.

[10] Z. Song, N. Yang, X. Lin, F. P. Delgado, H. Hofmann, and J. Sun, "Progression of cell-to-cell variation within battery modules under different cooling structures," *Applied Energy*, vol. 312, p. 118836, 2022.

[11] F. Jin and K. G. Shin, "Pack sizing and reconfiguration for management of large-scale batteries," in *2012 IEEE/ACM Third International Conference on Cyber-Physical Systems*. IEEE, 2012, pp. 138–147.

[12] J. Chen, L. Zhang, and W. Gao, "Reconfigurable model predictive control for large scale distributed systems," *IEEE Systems Journal*, vol. 18, no. 2, pp. 965–976, June 2024.

[13] T. Kim, W. Qiao, and L. Qu, "A series-connected self-reconfigurable multicell battery capable of safe and effective charging/discharging and balancing operations," in *2012 Twenty-Seventh Annual IEEE Applied Power Electronics Conference and Exposition (APEC)*. IEEE, 2012, pp. 2259–2264.

[14] F. Altaf, *Thermal and state-of-charge balancing of batteries using multilevel converters*. Chalmers Tekniska Hogskola (Sweden), 2014.

[15] J. Chen, A. Behal, Z. Li, and C. Li, "Active battery cell balancing by real time model predictive control for extending electric vehicle driving range," *IEEE Trans. Auto. Sci. Eng.*, vol. 21, no. 3, pp. 4003–4015, July 2024.

[16] Y. Weng and C. Ababei, "Ai-assisted reconfiguration of battery packs for cell balancing to extend driving runtime," *Journal of Energy Storage*, vol. 84, p. 110853, 2024.

[17] T. Morstyn, M. Momayyezan, B. Hredzak, and V. G. Agelidis, "Distributed control for state-of-charge balancing between the modules of a reconfigurable battery energy storage system," *IEEE Transactions on Power Electronics*, vol. 31, no. 11, pp. 7986–7995, 2015.

[18] S. Jeon, J. Kim, J. Ahn, and H. Cha, "Optimizing discharge efficiency of reconfigurable battery with deep reinforcement learning," *IEEE Transactions on Computer-Aided Design of Integrated Circuits and Systems*, vol. 39, no. 11, pp. 3893–3905, 2020.

[19] G. Gunlu, "Dynamically reconfigurable independent cellular switching circuits for managing battery modules," *IEEE Transactions on Energy Conversion*, vol. 32, no. 1, pp. 194–201, 2016.

[20] A. Škegro, C. Zou, and T. Wik, "Analysis of potential lifetime extension through dynamic battery reconfiguration," in *2023 25th European Conference on Power Electronics and Applications (EPE'23 ECCE Europe)*. IEEE, 2023, pp. 1–11.

[21] T. Kacetl, J. Kacetl, N. Tashakor, and S. M. Goetz, "Ageing mitigation and loss control through ripple management in dynamically reconfigurable batteries," *arXiv preprint arXiv:2211.03143*, 2022.

[22] D. N. How, M. Hannan, M. H. Lipu, and P. J. Ker, "State of charge estimation for lithium-ion batteries using model-based and data-driven methods: A review," *Ieee Access*, vol. 7, pp. 136 116–136 136, 2019.

[23] Y. Weng and C. Ababei, "Battery pack cell balancing using topology switching and machine learning," in *2022 IEEE Vehicle Power and Propulsion Conference (VPPC)*. IEEE, 2022, pp. 1–6.

[24] X. Lin, H. E. Perez, S. Mohan, J. B. Siegel, A. G. Stefanopoulou, Y. Ding, and M. P. Castanier, "A lumped-parameter electro-thermal model for cylindrical batteries," *Journal of Power Sources*, vol. 257, pp. 1–11, 2014.

[25] H. E. Perez, J. B. Siegel, X. Lin, A. G. Stefanopoulou, Y. Ding, and M. P. Castanier, "Parameterization and validation of an integrated electro-thermal cylindrical lfp battery model," in *Dynamic Systems and Control Conference*, vol. 45318. American Society of Mechanical Engineers, 2012, pp. 41–50.

[26] J. Chen, Z. Zhou, Z. Zhou, X. Wang, and B. Liaw, "Impact of battery cell imbalance on electric vehicle range," *Green Energy and Intelligent Transportation*, vol. 1, no. 3, p. 100025, 2022.

[27] T. N. Kipf and M. Welling, "Semi-supervised classification with graph convolutional networks," *arXiv preprint arXiv:1609.02907*, 2016.

[28] P. Veličković, G. Cucurull, A. Casanova, A. Romero, P. Lio, and Y. Bengio, "Graph attention networks," *arXiv preprint arXiv:1710.10903*, 2017.

[29] A. Irshayyid and J. Chen, "Highway merging control using multi-agent reinforcement learning," in *IEEE International Conference on Computing and Machine Intelligence (ICMI)*. IEEE, 2024, pp. 1–2.

[30] G. L. Plett, *Battery management systems, Volume II: Equivalent-circuit methods*. Artech House, 2015.